Applied Mathematical Biosystems, Volume 2, Issue 1, (Jan-Jun 2026), 1-8

Applied Mathematical Biosystems

journal homepage: https://ambjournal.com

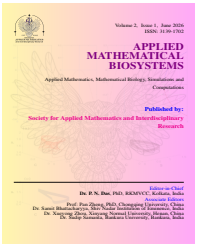

A Mathematical Model of Pneumococcal Infection Dynamics with Optimal Control Approach

Satyajeet Kumar[1], **Amar Nath Chatterjee**[2] **and Fahad Al Basir**[3]

[1]*Department of Mathematics, Magadh University, Bodh Gaya, Bihar, India*
[2]*Department of Mathematics, KLS College, Nawada, constituent unit of Magadh University, Bodh Gaya, Bihar, India*
[3]*Department of Mathematics, Asansol Girls' College, Asansol-4, West Bengal-713304, India*

Abstract

Pneumococcal infections is a serious threat for human health, which causes chronic and injurious respiratory disease problems. We provide a mathematical model that describes the interactions between three important populations in order to better understand the course of infection and the function of host immunity: the immune cell population (N), the bacterial population in the blood (B), and the pneumococcal bacteria in the lungs (P). Growth of bacteria, immune-mediated clearance, logistic restriction, and natural removal rates are all included in this proposed model. This model proposes insights into immune response efficiency, infection persistence, and probable treatment approaches by taking these processes. The foundation for future analytical investigation of equilibrium states, stability conditions, and intervention results in pneumococcal illness is laid by this work.

Keywords: *Modeling, Stability analysis, basic reproduction number, Optimal drug dosing, Numerical simulations*

Corresponding author: A. N. Chatterjee *E-mail address:* anchaterji@gmail.com
Received: April 5, 2026 **Revised:** May 28, 2026 **Accepted:** May 31, 2026 **Published:** June 14, 2026
© Jan-Jun 2026 Society for Applied Mathematics and Interdisciplinary Research **DOI:** 10.67029/j.amb.2026.0021.18

1. Introduction

Inflammation of the lungs is a necessary physiological reaction that may be generated by a broad range of insults, such as viral and bacterial infections, damage caused by mechanical ventilation, and exposure to harmful particles [1, 2]. Such illnesses are among of the most fatal internationally; for example, pneumonia is still one of the primary causes of mortality in children and the elderly [3]. The nature of the immune reaction, which includes a succession of signaling proteins such as cytokines, as well as distinct cell types such as macrophages, neutrophils, and T cells, makes it exceedingly challenging to judge the efficacy of therapies based just on clinical observation [4].

A serious health concern, pneumococcal infections can result in serious respiratory and systemic problems [5, 6]. Predicting the course of a disease and creating successful treatments need an understanding of the interactions between bacterial populations in the lungs, their dissemination into the bloodstream, and the immune system's reaction [7]. To tackle this complexity, mathematical modeling has become an important area of research to understand host-pathogen interactions [8, 9].

Mathematical models have been developed from simple ordinary differential equations (ODEs) to hybrid models that simulate the behaviour of host-pathogen interactions [9, 10]. By combining experimental results with mathematical models, researchers have been able to develop new approaches to treat diseases by testing biological hypotheses and understanding the role of important regulatory pathways [11]. To understand the function of drug dosing and co-infection with pathogens this process is carried out for several disease like influenza, pneumococcal pneumonia, and most recently, COVID-19 [12, 13].

Schirm et al [14] presents and analyzes a nonlinear ODE model of murine pneumococcal pneumonia that integrates bacterial dynamics, IL-6-driven inflammation, neutrophils/macrophages, tissue damage, and antibiotic action (ampicillin, moxifloxacin) to replicate time-series data and simulate treatment regimens. It identifies a stable pneumonia-free equilibrium with outcome bifurcation based on initial bacterial inocula and emphasizes the importance of early macrophage control, although pointing out the limitations of parameter identifiability. The paper [15] offers a nonlinear ODE model of murine pneumococcal pneumonia that is validated and demonstrates a bifurcation between clearance and persistent infection based on initial bacterial inocula, emphasizes early macrophage-mediated control and IL-6 dynamics, and illustrates the crucial role of early antibiotic treatment (ampicillin, moxifloxacin) in shaping outcomes, although again emphasizing the limitations of parameter identifiability. Smith et al [16] interestingly integrates how predictive mathematical modeling has significantly clarified influenza virus dynamics, immune regulation, and viral-bacterial co-infection mechanisms, emphasizing the value of model-

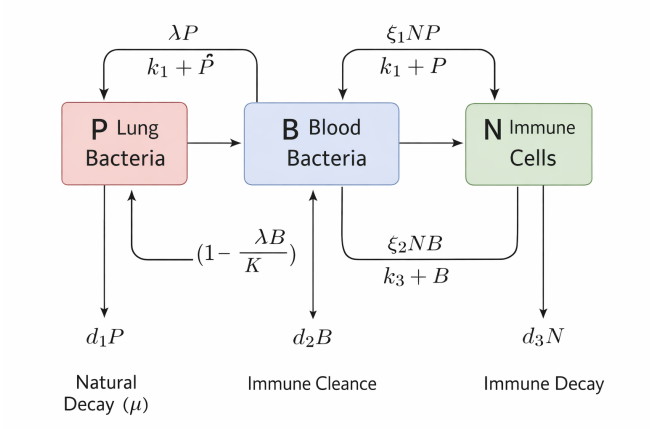

Figure 1. Schematic diagram for the model (4)

based experimental validation as a highly effective strategy to elucidate nonlinear host-pathogen interactions and therapeutic opportunities.

The innovative aspect of our analysis is its single framework that takes into account the dynamics of local infections along with their systemic counterparts in pneumococcal pneumonia. While the existing models, such as those of Schirm et al. [14], mainly dealt with murine pneumonia and immune dynamics in conjunction with antibiotic treatment, what distinguishes our model is our ability to combine these three compartments, namely, bacteria in the lungs, bacteria in the blood, and immune cells, each following its unique set of growth constraints and recruitment rules. Together with applying optimal control techniques to activate the immune response and fight the pathogen, we expand the scope of available knowledge by quantifying infection persistence levels, designing appropriate treatment methods, and conducting sensitivity analyses that are currently missing in the relevant literature.

In this study, our main objective is to formulate and analyse a mathematical model to get insight of the nonlinear dynamics of pneumococcal infection and host immune response so that we can design the possible investigation strategy in depth of the disease progression. Our mathematical model suggests a rigorous approach to analyse the interaction helps for clinical observations to unravel the complexity of bacterial growth, systemic spread, and immune regulation. Analysing the system of nonlinear ordinary differential equations, our study revels the equilibrium states, stability conditions and threshold for infection persistence versus clearance.

Also, the use of optimal control theory helps us to design and calculate therapeutic strategies, such as antibiotic administration and immune modulation, with the main target of minimization of bacteria along with treatment costs and side effects. The projected model also explains the biological mechanisms but also offers a quantitative basis for forecasting conclusions and controlling effective interference in pneumococcal disease.

2. Model Formulation

In this study, we present a system of nonlinear differential equations that captures the dynamics of three key populations:

(i) Pneumococcal bacteria in the lungs, P,
(ii) Bacterial population in the blood, B,
(iii) Immune cell population, N.

The model incorporates bacterial growth, immune-mediated clearance, and natural removal rates, providing a framework to analyze infection persistence, immune response efficiency, and possible therapeutic strategies.

We consider three coupled ordinary differential equations (ODEs) describing the time evolution of the system:

Pneumococcal Population in the Lungs is modeled using

$$\frac{dP}{dt} = \frac{\lambda_1 P}{k_1 + P} - \frac{\xi_1 NP}{k_1 + P} - d_1 P. \tag{1}$$

The first term represents bacterial growth with saturation constant k_1. The second term models phagocytosis by immune cells, proportional to both N and P. The last term accounts for natural removal or death rate of bacteria.

Blood Bacteria Population is modeled by the following equation

$$\frac{dB}{dt} = \lambda_2 B\left(1 - \frac{B}{K}\right) - \frac{\xi_2 NB}{k_3 + B} - d_2 B. \tag{2}$$

Logistic growth of bacteria in the bloodstream is modeled with carrying capacity K. Immune clearance occurs via phagocytosis, regulated by saturation constant k_3. Natural removal is represented by $d_2 B$.

Immune Cell Population is described as below:

$$\frac{dN}{dt} = \frac{\lambda_3 P}{k_4 + P} - d_3 N \tag{3}$$

Immune cell recruitment is stimulated by the presence of pneumococcal bacteria in the lungs, with saturation constant k_4. Natural decay or removal of immune cells is represented by $d_3 N$.

Thus, the dynamics of pneumococcal infection are described by the following system of nonlinear ordinary differential equations:

$$\begin{aligned}
\frac{dP}{dt} &= \frac{\lambda_1 P}{k_1 + P} - \frac{\xi_1 NP}{k_1 + P} - d_1 P, \\
\frac{dB}{dt} &= \lambda_2 B\left(1 - \frac{B}{K}\right) - \frac{\xi_2 NB}{k_3 + B} - d_2 B, \\
\frac{dN}{dt} &= \frac{\lambda_3 P}{k_4 + P} - d_3 N.
\end{aligned} \tag{4}$$

with initial population size $P(0) > 0, B(0) > 0, N(0) > 0$.

Remark 1. *In formulating the nonlinear system, several biological assumptions were made to capture the essential features of pneumococcal infection dynamics:*

(i) The replication of pneumococcal bacteria in lung tissue is limited by nutrient availability and host environmental constraints. To reflect this, we adopted a Michaelis–Menten type saturation term, which ensures that growth slows as bacterial density increases, consistent with biological observations.
(ii) The bloodstream is modeled as a constrained environment with a finite carrying capacity K. Logistic growth captures the balance between bacterial replication and systemic limitations, such as nutrient depletion and host defense mechanisms.
(iii) Clearance of bacteria in both lungs and blood is represented by saturating phagocytosis terms proportional to both bacterial and immune cell populations. This reflects the biological

Table 1. Model parameters, their biological meaning, and typical values [17, 18].

Symbol	Description	Value (Units)
P	Pneumococcal population in the lungs	– (cells)
B	Blood bacteria population	– (cells/mL)
N	Immune cell population	– (cells/mL)
λ_1	Growth rate of lung bacteria	0.5 (day^{-1})
λ_2	Logistic growth rate of blood bacteria	0.3 (day^{-1})
λ_3	Growth rate of immune cells	0.25 (day^{-1})
k_1, k_2	Saturation constants	2×10^3 (cells)
k_3, k_4	Saturation constants	2×10^3 (cells)
ξ_1	Phagocytosis rate in lungs	0.05 (day^{-1})
ξ_2	Phagocytosis rate in blood	$0.01 - 0.1$ (day^{-1})
d_1, d_2, d_3	Removal rates	0.1 (day^{-1})
K	Carrying capacity of blood bacteria	10^6 (cells/mL)

process where immune cells engulf bacteria, but clearance efficiency is limited by binding and engulfment capacity.

(iv) Recruitment of immune cells is assumed to be triggered primarily by lung infection. This assumption is based on biological evidence that pulmonary infection initiates systemic immune activation, while blood bacteria alone do not directly stimulate recruitment at the same level.

These assumptions provide a biologically grounded framework for analyzing infection persistence, immune response efficiency, and therapeutic strategies. By explicitly modeling saturation, logistic restriction, and compartment-specific recruitment, the system captures both local and systemic aspects of pneumococcal infection.

3. Equilibrium analysis

The system (4) has three equilibria, namely

(i) The Disease-free equilibrium (DFE) corresponds to the absence of infection. Setting $P = 0$, $B = 0$, and $N = 0$, the system reduces to:

$$(P_0, B_0, N_0) = (0, 0, 0).$$

(ii) $E_1(P_1, B_1, N_1) = \left(P_1,\ 0,\ \frac{\lambda_3 P_1}{d_3(k_4+P_1)}\right)$, where P_1 is given by the quadratic formula:

$$P_1 = \frac{(\lambda_1 d_3 - \xi_1\lambda_3) - d_1 d_3(k_1 + k_4) \ \pm\ \sqrt{D}}{2d_1 d_3}.$$

$$D = \Big(d_1 d_3(k_1 + k_4) - (\lambda_1 d_3 - \xi_1\lambda_3)\Big)^2 - 4d_1 d_3\big(d_1 d_3 k_1 k_4 - \lambda_1 d_3 k_4\big).$$

(iii) The endemic equilibrium corresponds to a steady state with persistent infection, i.e. $P^* > 0$, $B^* > 0$, and $N^* > 0$. Setting the right-hand sides of the system (4) to zero, we obtain the endemic equilibrium $E^*(P^*, B^*, N^*)$, where

$$N^* = \frac{\lambda_3 P^*}{d_3(k_4 + P^*)},$$

$$B^* = \frac{\left[(\lambda_2 - d_2) - \frac{\lambda_2}{K}k_3\right] \pm \sqrt{D_1}}{2\lambda_2/K},$$

where

$$P^* = \frac{\left[d_3(\lambda_1 - d_1(k_1 + k_4)) - \xi_1\lambda_3\right] \pm \sqrt{D_2}}{2d_3 d_1}.$$

where, $D_1 = \left[(\lambda_2 - d_2) - \frac{\lambda_2}{K}k_3\right]^2 + \frac{4\lambda_2}{K}\left((\lambda_2 - d_2)k_3 - \frac{\xi_2\lambda_3 P^*}{d_3(k_4+P^*)}\right)$,

and $D_2 = \left[d_3(\lambda_1 - d_1(k_1 + k_4)) - \xi_1\lambda_3\right]^2 + 4d_3 d_1(\lambda_1 - d_1 k_1)k_4$.

It is observed that the quadratic expression for P^* yields two potential solutions. However, only the positive root ensuring $P^* > 0$, $N^* > 0$, and $B^* > 0$ is considered biologically relevant.

4. The Basic Reproduction Number

We analyze the system using the Next Generation Matrix (NGM) method to determine the disease-free equilibrium (DFE) and the basic reproduction number R_0.

We identify the infection compartments as P (bacteria in lungs) and B (bacteria in blood). The immune cells N are not infectious but act as a response.

Expanding the system near the DFE:

$$\frac{dP}{dt} \approx \frac{\lambda_1}{k_1}P - d_1 P,$$

$$\frac{dB}{dt} \approx \lambda_2 B - d_2 B,$$

$$\frac{dN}{dt} \approx \frac{\lambda_3}{k_4}P - d_3 N.$$

We separate the system into new infection terms F and transition terms V as:

$$F = \begin{bmatrix} \frac{\lambda_1}{k_1}P \\ \lambda_2 B \end{bmatrix}, \quad V = \begin{bmatrix} d_1 P \\ d_2 B \end{bmatrix}.$$

Thus, the Jacobian matrices at the DFE are:

$$F = \begin{bmatrix} \frac{\lambda_1}{k_1} & 0 \\ 0 & \lambda_2 \end{bmatrix}, \quad V = \begin{bmatrix} d_1 & 0 \\ 0 & d_2 \end{bmatrix}.$$

Thus the next generation matrix is:

$$K = FV^{-1} = \begin{bmatrix} \frac{\lambda_1}{d_1 k_1} & 0 \\ 0 & \frac{\lambda_2}{d_2} \end{bmatrix}.$$

The basic reproduction number R_0 is the spectral radius of K:

$$R_0 = \max\left(\frac{\lambda_1}{d_1 k_1}, \frac{\lambda_2}{d_2}\right).$$

We now analyze the stability of the disease-free equilibrium (DFE) using the basic reproduction number R_0 obtained via the Next Generation Matrix method.

5. Stability analysis

Here, we present the stability analysis of equilibrium points.

5.1. Stability of DFE

The Jacobian matrix of the system is obtained by differentiating the right-hand sides of the system with respect to (P, B, N):

$$J(P,B,N) = \begin{bmatrix} J_{11} & 0 & -\frac{\xi_1 P}{k_1+P} \\ 0 & \lambda_2\left(1-\frac{2B}{K}\right) - \frac{\xi_2 N k_3}{(k_3+B)^2} - d_2 & -\frac{\xi_2 B}{k_3+B} \\ \frac{\lambda_3 k_4}{(k_4+P)^2} & 0 & -d_3 \end{bmatrix},$$

where $J_{11} = \frac{\lambda_1 k_1}{(k_1+P)^2} - \frac{\xi_1 N k_1}{(k_1+P)^2} - d_1$. The Jacobian matrix of the system at $(P_0, B_0, N_0) = (0,0,0)$ has eigenvalues as:

$$\rho_1 = \frac{\lambda_1}{k_1} - d_1, \quad \rho_2 = \lambda_2 - d_2, \quad \rho_3 = -d_3.$$

The immune cell eigenvalue $\rho_3 = -d_3 < 0$ is always negative. Other two eigenvalues, $\rho_1 < 0$ and $\rho_2 < 0$, if

$$\frac{\lambda_1}{d_1 k_1} < 1, \quad \frac{\lambda_2}{d_2} < 1.$$

Recall that

$$R_0 = \max\left(\frac{\lambda_1}{d_1 k_1}, \frac{\lambda_2}{d_2}\right).$$

Thus if $R_0 < 1$, all eigenvalues are negative and the DFE is locally asymptotically stable. The infection dies out. If $R_0 > 1$, at least one eigenvalue is positive and the DFE is unstable. Thus we have the following theorem.

Theorem 1. *The stability of the disease-free equilibrium is completely determined by the basic reproduction number R_0. The DFE is stable when $R_0 < 1$ and unstable when $R_0 > 1$.*

5.2. Stability of E^*

At the endemic equilibrium (P^*, B^*, N^*), the Jacobian becomes:

$$J^* = \begin{bmatrix} a_{11} & 0 & a_{13} \\ 0 & a_{22} & a_{23} \\ a_{31} & 0 & a_{33} \end{bmatrix},$$

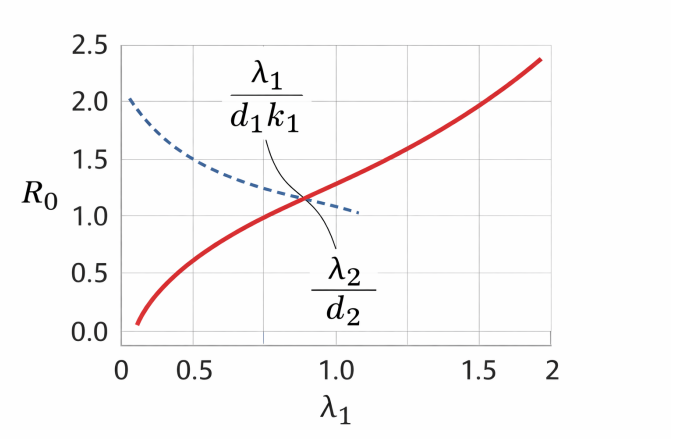

Figure 2. Bifurcation diagram showing the fundamental reproductive number R_0 in relation to the lung bacterial growth rate (λ_1). This bifurcation diagram shows how variations in λ_1 affect the stability of the pneumococcus infection system. The point of crossing denotes the change from infection elimination to infection establishment, and the two branches depict the competition between germs developing in the blood and lungs.

where

$$a_{11} = \frac{\lambda_1 k_1}{(k_1+P^*)^2} - \frac{\xi_1 N^* k_1}{(k_1+P^*)^2} - d_1,$$

$$a_{13} = -\frac{\xi_1 P^*}{k_1+P^*},$$

$$a_{22} = \lambda_2\left(1-\frac{2B^*}{K}\right) - \frac{\xi_2 N^* k_3}{(k_3+B^*)^2} - d_2,$$

$$a_{23} = -\frac{\xi_2 B^*}{k_3+B^*},$$

$$a_{31} = \frac{\lambda_3 k_4}{(k_4+P^*)^2},$$

$$a_{33} = -d_3.$$

The characteristic equation is determined using

$$\det(J^* - \rho I) = \det\begin{bmatrix} a_{11}-\rho & 0 & a_{13} \\ 0 & a_{22}-\rho & a_{23} \\ a_{31} & 0 & a_{33}-\rho \end{bmatrix}.$$

Expanding along the second column:

$$\det(J^* - \rho I) = (a_{22}-\rho)\det\begin{bmatrix} a_{11}-\rho & a_{13} \\ a_{31} & a_{33}-\rho \end{bmatrix}.$$

$$= (a_{22}-\rho)\big[(a_{11}-\rho)(a_{33}-\rho) - a_{13}a_{31}\big].$$

Characteristic Equation

$$(\rho - a_{22})\big(\rho^2 - (a_{11}+a_{33})\rho + a_{11}a_{33} - a_{13}a_{31}\big) = 0.$$

Thus the eigenvalues are:

$\rho_1 = a_{22}$, $\rho_{2,3}$ are roots of $\rho^2 - (a_{11}+a_{33})\rho + (a_{11}a_{33} - a_{13}a_{31}) = 0$.

For local stability, all eigenvalues must have negative real parts.

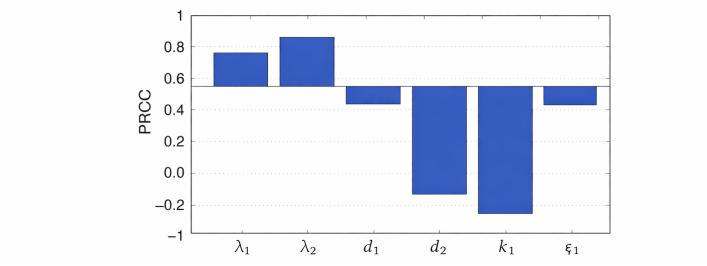

Figure 3. Partial rank correlation coefficient (PRCC) graph for the sensitivity analysis of R_0. Bars show the partial rank correlation coefficient (PRCC) between R_0 and significant factors (λ_1, λ_2, d_1, d_2, k_1, ξ_1), emphasizing the positive effect of bacterial proliferation rates and the negative effect of decay and clearance rates.

The conditions for negative real parts are obtained by using Routh-Hurwitz criteria as:

$$a_{22} < 0, \qquad a_{11} + a_{33} < 0, \qquad a_{11}a_{33} - a_{13}a_{31} > 0.$$

Thus,we have the following theorem.

Theorem 2. *The endemic equilibrium is asymptotically stable if the following conditions are satisfied:*

$$a_{22} < 0, \quad a_{11} + a_{33} < 0, \quad a_{11}a_{33} - a_{13}a_{31} > 0. \tag{5}$$

6. Optimal control Problem

In this section our main aim is to minimize the cost as well as minimize the blood bacteria population. We construct the optimal control problem where the state system is

$$\begin{aligned}
\frac{dP}{dt} &= \frac{\lambda_1 P}{k_1 + P} - \frac{\xi_1 NP}{k_1 + P} - d_1 P, \\
\frac{dB}{dt} &= \lambda_2 B\left(1 - \frac{B}{K}\right) - \frac{\xi_2 NB}{k_3 + B} - d_2 B, \\
\frac{dN}{dt} &= (1 - u(t))\omega + \frac{\lambda_3 P}{k_4 + P} - d_3 N.
\end{aligned} \tag{6}$$

and the control function $u(t)$ represents the efficacy of immune activator therapy, modulating immune recruitment.

The objective function is assumed as

$$J(u) = \int_{t_i}^{t_f} [A_1 u^2 + A_2 B^2 + A_3 N^2] dt \tag{7}$$

The parameters A_1, A_2 and A_3 are the weight on the benefit of the cost. These are the cost of per unit of immune activator. Here the control $u(t)$ represents the efficacy of immune activator therapy. In this problem we are seeking the optimal control $u(t)$ such that

$$J(u^*) = \min\{J(u) : u \in U\}. \tag{8}$$

Here U is the control set defined by $U = \{u(t) : u \text{ is measurable}, 0 \le u(t) \le 1, t \in [t_i, t_f]\}$.

To determine the optimal control u^*, we use the 'Pontryagin Minimum Principle' [19]. To solve the problem, we use the Hamiltonian [20] given by

$$\begin{aligned}
\mathcal{H} = {} & A_1 u^2 - A_2 B^2 + A_3 N^2 + \rho_1\{\frac{\lambda_1 P}{k_1 + P} - \frac{\xi_1 NP}{k_1 + P} - d_1 P\} \\
& + \rho_2\{\lambda_2 B\left(1 - \frac{B}{K}\right) - \frac{\xi_2 NB}{k_3 + B} - d_2 B\} \\
& + \rho_3\{u(t)\omega + \frac{\lambda_3 P}{k_4 + P} - d_3 N\}
\end{aligned} \tag{9}$$

6.1. Existence of a unique optimal control

To establish the existence of an optimal control $u^*(t)$ for the problem defined above, we verify the standard conditions from optimal control theory. The admissible control set is given by

$$U = \{u(t) : u(t) \text{ is measurable}, 0 \le u(t) \le 1, t \in [t_i, t_f]\}.$$

This set is nonempty, convex, and closed. The state system is bilinear in the state and control variables, with right-hand sides that are continuously differentiable and satisfy Lipschitz continuity in (P, B, N), ensuring the existence of unique solutions for each admissible control.

The integrand of the objective functional,

$$L(P, B, N, u) = A_1 u^2 + A_2 B^2 + A_3 N^2,$$

is convex in u and bounded below by zero. Furthermore, the state equations guarantee bounded trajectories for (P, B, N) over the finite time horizon $[t_i, t_f]$. By standard results [21], these conditions imply the existence of an optimal control $u^*(t)$ that minimizes $J(u)$.

Uniqueness of the optimal control follows from the strict convexity of the integrand in u, since $A_1 > 0$ ensures that $L(P, B, N, u)$ is strictly convex with respect to u. Therefore, the optimal control $u^*(t)$ is unique.

6.2. Characterize the optimal control

By using the 'Pontryagin Minimum Principle' and for the existence condition of the optimal control theory [22], we obtain the following theorem.

Theorem 3. *The objective cost function $J(u)$ over U is minimum for the optimal control u^* corresponding to the endemic equilibrium (P^*, B^*, N^*). Also there exist adjoint function ρ_1, ρ_2, ρ_3 satisfying the following Equations:*

$$\begin{cases}
\dot{\rho}_1 &= -\rho_1\left(\frac{\lambda_1 k_1}{(k_1+P)^2} - \frac{\xi_1 N k_1}{(k_1+P)^2} - d_1\right) - \rho_3 \frac{\lambda_3 k_4}{(k_4+P)^2}, \\
\dot{\rho}_2 &= -\left(2A_2 B + \rho_2\left(\lambda_2\left(1 - \frac{2B}{K}\right) - \frac{\xi_2 N k_3}{(k_3+B)^2} - d_2\right)\right), \\
\dot{\rho}_3 &= -\left(2A_3 N - \rho_1 \frac{P}{k_1+P} - \rho_2 \frac{B}{k_3+B} - \rho_3 d_3\right).
\end{cases} \tag{10}$$

Proof. The adjoint variables satisfy

$$\dot{\rho}_i = -\frac{\partial \mathcal{H}}{\partial x_i}, \quad x_1 = P, \ x_2 = B, \ x_3 = N.$$

Thus,

$$\dot{\rho}_1 = -\frac{\partial \mathcal{H}}{\partial P}, \quad \dot{\rho}_2 = -\frac{\partial \mathcal{H}}{\partial B}, \quad \dot{\rho}_3 = -\frac{\partial \mathcal{H}}{\partial N}. \tag{11}$$

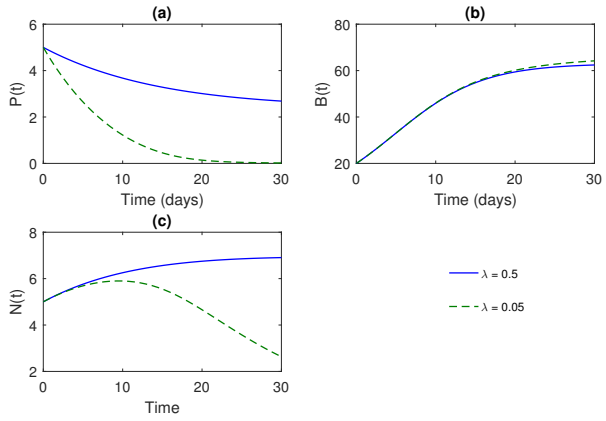

Figure 4. Time evolution of dynamics of pneumococcal infection for various growth rates of bacteria (λ). Graphs illustrate the dynamics of (a) population of pneumococci in lungs $P(t)$, (b) population of bacteria in blood $B(t)$, and (c) population of immune cells $N(t)$ for two sets of parameters, $\lambda = 0.5$ (blue solid line) and $\lambda = 0.05$ (dashed green line).

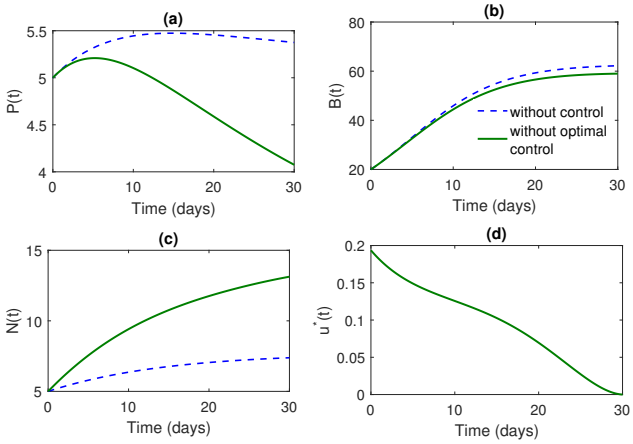

Figure 5. Comparison between dynamics of pneumococcus infection model under and without optimal control. Plots depicting the dynamics of (a) $P(t)$ the bacteria density in lungs, (b) $B(t)$ the bacteria density in blood, (c) $N(t)$ the immune cells density, and (d) $u^*(t)$, the control. Dashed blue line corresponds to no control, whereas green solid lines depict optimal control.

This give the following system:

$$\dot{\rho}_1 = -\rho_1\left(\frac{\lambda_1 k_1}{(k_1+P)^2} - \frac{\xi_1 N k_1}{(k_1+P)^2} - d_1\right) - \rho_3\frac{\lambda_3 k_4}{(k_4+P)^2},$$

$$\dot{\rho}_2 = -\left(-2A_2B + \rho_2\left(\lambda_2\left(1-\frac{2B}{K}\right) - \frac{\xi_2 N k_3}{(k_3+B)^2} - d_2\right)\right),$$

$$\dot{\rho}_3 = -\left(2A_3N - \rho_1\frac{P}{k_1+P} - \rho_2\frac{B}{k_3+B} - \rho_3 d_3\right).$$

The optimal control is obtained from below relation:

$$\frac{\partial \mathcal{H}}{\partial u} = 0.$$

This gives,

$$\frac{\partial \mathcal{H}}{\partial u} = 2A_1u - \xi_3\omega.$$

Hence,

$$u(t) = \frac{\xi_3(t)\,\omega}{2A_1}.$$

Since $u(t) \in [0,1]$, the optimal control is given by

$$u^*(t) = \min\left\{1, \max\left\{0, \frac{\xi_3(t)\,\omega}{2A_1}\right\}\right\}. \tag{12}$$

The adjoint system is given by the three costate equations above. The optimal control is expressed as a projection of $\frac{\xi_3\omega}{2A_1}$ onto the admissible set $[0,1]$. □

7. Numerical simulations

Figure 2 represents the bifurcation analysis of the connection between the basic reproduction number R_0 and the lung bacterial growth rate constant λ_1. As shown by the graph, an increase in λ_1 results in a nonlinear increase in R_0, thus implying an increased possibility for infection as a result of a higher rate of bacteria growth in the lungs. These two branches denote the values $\frac{\lambda_1}{d_1 k_1}$ and $\frac{\lambda_2}{d_2}$. The former is concerned with the lung bacteria growth, while the latter deals with the blood bacteria population. The point of their intersection is where the basic reproduction number is equal to 1, indicating the start of an infection spread process.

The PRCC plots (see figure 3) show how changes in the parameter values influence the basic reproduction number R_0. A positive correlation between λ_1 and λ_2 and R_0 implies that an increase in the bacterial growth rates in both lungs and bloodstream leads to a significant increase in R_0 thus favoring the maintenance of the infection. On the other hand, the negative correlation between d_1, d_2, and k_1 and R_0 implies that increasing the rate at which bacteria are cleared from the body and carrying capacity decreases R_0. The positive effect of ξ_1 on R_0 implies that immune clearance is more complicated and may balance the growth rate. In summary, bacterial growth rates play a significant role in the dynamics of the infection while natural decay and immunity clearance stabilize the system to prevent infections.

Figure 4 represents the effect of changing bacterial growth rate (λ) on the infection progression within various body parts due to pneumococcal bacteria. From Figure 4 (a), it is evident that the number of bacteria in the lung decreases with time; however, it happens at a faster rate when $\lambda = 0.05$. This implies that a lower bacterial growth rate leads to faster clearance of bacteria from the lung. Figure 4 (b) represents the number of bacteria in the blood, where we observe an increase to a certain equilibrium value despite a lower bacterial growth rate within the lungs. The close proximity of the two graphs indicates that the dynamics of bacteria within the blood system are not very sensitive to changes in λ. Figure 4 (c) shows the number of immune cells within the host system, where the number increases with the onset of infection. When the bacterial growth rate within the lungs is high, there is sustained immune activation, but otherwise, a reduction in the bacterial population leads to decreased immune activation due to low stimulation.

The diagram 5 above emphasizes the effect of optimal control measures on the dynamics of pneumococcal infections. As seen in Figure 5 (a), the population of bacteria in the lungs ($P(t)$) first increases but is then suppressed efficiently through optimal control measures. This confirms the effectiveness of optimal control measures in inhibiting bacterial population. The second

Figure 5 (b) shows that the population of bacteria in the blood also increases in both cases, but with the optimal control measures, the bacteria population remains relatively low. In Figure 5 (c), the recruitment of the immune cells is depicted. It can be observed that the immune response recruitment rate is higher and sustained under optimal control, while without control, the recruitment takes time to kick off. Finally, Figure 5 (d) shows the control measures ($u^*(t)$), which start at a low level and gradually decline over time.

8. Discussion

By combining bacterial growth, immune response, and bacterial clearance, the mathematical model in this article has been able to effectively depict the nonlinear dynamical behavior of the pneumococcus infection. The mathematical model shows how local and systemic infection behaviors interact by classifying bacteria into two groups: blood bacteria and lung bacteria. According to the equilibrium and stability study, the fundamental reproduction number R_0 either initiates infection or eliminates the bacterium. The germs are totally eradicated when $R_0 < 1$, but the illness becomes endemic when $R_0 > 1$.

The impact of changing the parameter λ_1 on R_0 is observed in the bifurcation analysis displayed in Figure 2. The sensitivity of infection persistence is indicated by the nonlinear variation in R_0 with increasing λ_1. The threshold at which the infection can be eradicated or established is the point where the branches of the bifurcation intersect.

Finding the most significant factors influencing R_0 is further made easier by using the PRCC plot (Figure 3) for the sensitivity analysis. The positive association between λ_1 and λ_2 indicates that the likelihood of infection increases when bacterial growth rates rise in both compartments. Increases in decay and clearance rates decrease the likelihood of infection because of the negative correlations between d_1, d_2, and k_1. The complicated nature of immunological clearance is revealed by the moderately beneficial impact of ξ_1.

The dynamics of infection development and control measures are depicted in the numerical simulations (Figures 4 and 5). Low bacterial growth rates lead to rapid clearance in the lung compartment, low immune cell activation, and high bacterial counts in the blood compartment, as shown in Figure 4. This indicates that the sensitivity of the blood compartment bacterial population growth rate in the lungs is limited. The impact of optimum control methods on bacterial infections is seen in Figure 5, where therapy results in an increase in immune cells and a decrease in bacterial populations in the blood and lungs. Over time, the control parameter $u^*(t)$ diminishes, indicating decreased treatment effectiveness.

9. Conclusion

This article offers a mathematical model that explains the dynamics of pneumococcal infections and their treatments. Analytical study enables us to determine the equilibrium and stability analysis. Here the basic reproduction number R_0 plays an important role in determining the infection dynamics, while the bifurcation and sensitivity analysis show bacterial growth and removal parameters affect disease progression. Numerical findings show that an optimal control strategy plays a crucial role in setting the antibiotic or immune modulator strategy, which helps to reduce the bacterial levels and increase immunity levels to make the system reach a disease-free equilibrium state.

From this study we can predict that the effective treatment can be applied on time and can help to avoid further bacterial proliferation and systemic propagation. The analytical and numerical simulations can be used to develop treatment strategies and also help for experimental validation of the model. We can extend our work by formulating a stochastic model by incorporating co-infection with other bacteria of drug resistance in order to increase its relevance to the clinic.

Declarations

Acknowledgement: We would like to thank reviewers for their valuable comments and suggestions to improve the quality of the article.
Authors' Contributions: All authors are equally contributed to write the article.
Funding: There is no fund available for this work.
Conflict of Interest: The authors have no conflict of interest.
Use to AI Tools: We have used Gramerraly to check and correct the similarity and grammatical mistakes.

REFERENCES

[1] B Moldoveanu, P Otmishi, P Jani, J Walker, X Sarmiento, J Guardiola, M Saad, and Jerry Yu. Inflammatory mechanisms in the lung. *Journal of inflammation research*, pages 1–11, 2008.

[2] Nicola Clementi, Sreya Ghosh, Maria De Santis, Matteo Castelli, Elena Criscuolo, Ivan Zanoni, Massimo Clementi, and Nicasio Mancini. Viral respiratory pathogens and lung injury. *Clinical microbiology reviews*, 34(3):10–1128, 2021.

[3] Kim Mulholland. Childhood pneumonia mortality—a permanent global emergency. *The Lancet*, 370(9583):285–289, 2007.

[4] Carl Nathan. Neutrophils and immunity: challenges and opportunities. *Nature reviews immunology*, 6(3):173–182, 2006.

[5] E Ludwig, Paolo Bonanni, G Rohde, A Sayiner, and A Torres. The remaining challenges of pneumococcal disease in adults. *European Respiratory Review*, 21(123):57–65, 2012.

[6] Kim Mulholland. Strategies for the control of pneumococcal diseases. *Vaccine*, 17:S79–S84, 1999.

[7] Arnaud Didierlaurent, John Goulding, and Tracy Hussell. The impact of successive infections on the lung microenvironment. *Immunology*, 122(4):457–465, 2007.

[8] Denise E Kirschner and Jennifer J Linderman. Mathematical and computational approaches can complement experimental studies of host–pathogen interactions. *Cellular microbiology*, 11(4):531–539, 2009.

[9] Jan Ewald, Patricia Sieber, Ravindra Garde, Stefan N Lang, Stefan Schuster, and Bashar Ibrahim. Trends in mathematical modeling of host–pathogen interactions. *Cellular and Molecular Life Sciences: CMLS*, 77(3):467, 2019.

[10] Priti Kumar Roy, Jayanta Mondal, Sourav Rana, and Abhirup Datta. Host pathogen interactions with recovery rate using fractional-order derivative: A mathematical approach. *Nonlinear Studies*, 20(2):251–261, 2013.

[11] Hans Peter Fischer. Mathematical modeling of complex biological systems: from parts lists to understanding systems behavior. *Alcohol Research & Health*, 31(1):49, 2008.

[12] Amar Nath Chatterjee, Fahad Al Basir, Dibyendu Biswas, and Teklebirhan Abraha. Global dynamics of sars-cov-2

infection with antibody response and the impact of impulsive drug therapy. *Vaccines*, 10(11):1846, 2022.

[13] K Sreenath, Priyam Batra, EV Vinayaraj, Ridhima Bhatia, KVP SaiKiran, Vishwajeet Singh, Sheetal Singh, Nishant Verma, Urvashi B Singh, Anant Mohan, et al. Coinfections with other respiratory pathogens among patients with covid-19. *Microbiology spectrum*, 9(1):10–1128, 2021.

[14] Sibylle Schirm, Peter Ahnert, Sandra Wienhold, Holger Mueller-Redetzky, Geraldine Nouailles-Kursar, Markus Loeffler, Martin Witzenrath, and Markus Scholz. A biomathematical model of pneumococcal lung infection and antibiotic treatment in mice. *PLOS ONE*, 11(5):e0156047, 2016.

[15] Sarah B. Minucci, Rebecca L. Heise, and Angela M. Reynolds. Review of mathematical modeling of the inflammatory response in lung infections and injuries. *Frontiers in Applied Mathematics and Statistics*, 6:36, 2020.

[16] Amber M. Smith. Host–pathogen kinetics during influenza infection and coinfection: insights from predictive modeling. *Immunological Reviews*, 285(1):97–112, 2018.

[17] Nuwayyir Almutairi and Moustafa El-Shahed. Optimal control strategies for a mathematical model of pneumonia infection. *Computation*, 13(9):204, 2025.

[18] Timothy Kiprono Yano and Jacob Bitok. Computational modelling of pneumonia disease transmission dynamics with optimal control analysis. *Applied and Computational Mathematics*, 11(5):130–139, 2022.

[19] Lev Semenovich Pontryagin. *Mathematical theory of optimal processes*. Routledge, 2018.

[20] Morton I Kamien, Nancy L Schwartz, et al. Dynamic optimization: the calculus of variations and optimal control in economics and management. *Advanced textbooks in economics*, 31, 1980.

[21] Wendell Fleming and Raymond Rishel. The optimal control problem. In *Deterministic and Stochastic Optimal Control*, pages 20–59. Springer, 1975.

[22] Wendell H Fleming and Raymond W Rishel. *Deterministic and stochastic optimal control*. Springer Science & Business Media, 2012.